Title

Development of small particle speciation for nuclear forensics by soft X-ray scanning transmission spectromicroscopy

Journal

Analyst, 143(6)

ISSN

0003-2654

Authors

Pacold, JI

Altman, AB

Knight, KB

et al.

Publication Date

2018-03-12

DOI

10.1039/c7an01838j

Analytical Methods

ARTICLE

Development of Small Particle Speciation for Nuclear Forensics by Soft X-ray Scanning Transmission Spectromicroscopy

Received 00th January 20xx,
Accepted 00th January 20xx

DOI: 10.1039/x0xx00000x

www.rsc.org/

J. I. Pacold,[a] A. B. Altman[a,b], K. B. Knight,[c] K. S. Holliday,[d] M. J. Kristo,[c] S. G. Minasian,[a] T. Tyliszczak,[e] C. H. Booth,[a] and D. K. Shuh[a*]

Synchrotron radiation spectromicroscopy provides a combination of submicron spatial resolution and chemical sensitivity that is well-suited to analysis of heterogeneous nuclear materials. The chemical and physical characteristics determined by scanning transmission X-ray microscopy (STXM) are complementary to information obtained from standard radiochemical analysis methods. In addition, microscopic quantities of radioactive material that cannot be analyzed rapidly and directly by existing forensic methodologies can be characterized rapidly by STXM with minimal sample handling and intrusion, especially in the case of particulate materials. The STXM can accommodate a diverse range of samples including wet materials, complex mixtures, and small quantities of material contained in a larger matrix. In these cases, the inventory of species present in a samples is likely to carry information on its process history; STXM has the demonstrated capability to identify contaminants and sample matrices. Operating in the soft X-ray regime provides particular sensitivity to the chemical state of specimens containing low-*Z* materials, via the K-edges of light elements. Here, recent developments in forensics-themed spectromicroscopy, sample preparation, and data acquisition methods at the Molecular Environmental Science Beamline 11.0.2 of the Advanced Light Source are described. Results from several initial studies are presented, demonstrating the capability to identify the distribution of the species present in heterogeneous uranium-bearing materials. Future opportunities for STXM forensic studies and potential methodology development are discussed.

1. Introduction

Nuclear forensic analysis is concerned with physical and chemical signatures that can provide information about the source and process history of a sample of unidentified nuclear material.[1-3] Signatures such as the presence and concentration of chemical impurities, sample morphology, and the isotopics of U, Pu, and trace elements have been identified in the literature and associated with steps in the sample history.[4-8] Sample morphology, for example, can be associated with the intended use of the material (e.g., the reactor type in the case of a nuclear fuel sample).[9] Isotopic content and trace element impurities can be correlated with process history, and in some cases can provide information on the possible geographic origin of a specimen.[10-13]

Data from a broad array of analytical methods are typically needed to completely characterize a forensic specimen, with each measurement providing a different constraint on the possible process history and origin. Techniques applied in the literature include mass spectrometry, nuclear counting, X-ray fluorescence, and powder X-ray diffraction. As forensic specimens are often heterogeneous and morphology can provide important information on process history, it is essential to also use microanalytical methods, such as scanning electron microscopy (SEM)/energy–dispersive X-ray spectroscopy (EDS), transmission electron microscopy (TEM) and nanoscale secondary ion mass spectrometry (nano-SIMS).[14-18] While X-ray absorption spectroscopy has been applied to a limited number of materials of forensic interest.[19-23] The sensitivity of X-ray absorption near edge structure (XANES) to oxidation state lends itself to the observation of the gradual oxidation of nuclear material due to storage and environmental conditions,[23-24] and to studies of chemical signatures of post-detonation material.[25-26] This article describes the use of scanning transmission X-ray microscopy (STXM) in the soft X-ray region with methods optimized for nondestructive nuclear forensic analysis.

STXM combines 25 nm or finer spatial resolution with the nondestructive chemical sensitivity of XANES. This yields spectroscopic data that is complementary to other spatial data

[a] *Chemical Sciences Division, Lawrence Berkeley National Laboratory, Berkeley, CA 94720, USA*
[b] *Department of Chemistry, University of California, Berkeley, California 94720, USA*
[c] *Nuclear and Chemical Sciences Division, Lawrence Livermore National Laboratory, Livermore, California 94550, USA*
[d] *Materials Science Division, Lawrence Livermore National Laboratory, Livermore, California 94550, USA*
[e] *Advanced Light Source, Lawrence Berkeley National Laboratory, Berkeley, CA 94720, USA*
* Corresponding author; email dkshuh@lbl.gov

such as the elemental distributions provided by SEM/EDS and the isotopic information available from nano-SIMS. The spatial resolution of STXM makes it possible to work with microgram or less quantities of material. Operation in the soft X-ray regime provides access to both the actinide $N_{4,5}$-edges and the K-edges of light atoms, particularly C, N, O, and F. This is an important feature for analysis of nuclear materials since in the case of actinide materials the light atom edges are often more sensitive than the metal edges to variations in oxidation state and bonding.[27-30]

Rapid turnaround is desirable in forensic studies, particularly when the same sample must be examined using a large number of different methods. Past studies of illicit nuclear material have required a combination of rapid analyses at several different facilities to rule out possible origins of the material.[10-11] Here, technical developments in sample preparation and instrument operation at the Molecular Environmental Science (MES) STXM Beamline 11.0.2 of the Advanced Light Source (ALS) are described, with a focus on improved utility and throughput for heterogeneous forensic specimens. Initial results are presented, including baseline spectra acquired from common uranium materials, demonstrations of STXM speciation capability on mixtures of known particulates, and preliminary studies of forensic specimens. Additional future developments are discussed with a view towards improved integration of STXM into the suite of existing nuclear forensic analysis methods.

2. Technical Developments at Advanced Light Source Beamline 11.0.2

2.1 Instrument Description

The MES STXM (Fig. 1) is located on one of the two MES Beamline 11.0.2 branchlines of the ALS at Lawrence Berkeley National Laboratory.[31] The general design and operation principles of the STXM instruments and additional details on the MES STXM at the ALS in particular have been reported previously.[32-34] In brief, the MES beamline provides a regular operational energy range from approximately 120 eV to 2000 eV and a resolving power (E/ΔE) greater than 7500. X-ray zone plates and interferometer-controlled sample positioning stages are used to enable imaging with spatial resolution better than 25 nm. Images are usually acquired by rastering a sample through the focused X-ray beam and monitoring the transmitted intensity with a photomultiplier or photodiode. As discussed further in Section 2.2, a silicon drift detector may be installed to acquire X-ray fluorescence images. Stacks of images collected over a range of photon energies can be processed to extract spatially resolved spectroscopic data.

The ALS electron storage ring and the MES beamline operate under ultra-high vacuum (UHV, less than 10^{-9} Torr), but the STXM sample chamber can operate under lower vacuum (approximately 10^{-7} Torr) or He at ambient pressure, as the photon beam enters the chamber through a 50 nm Si_3N_4 isolation window. Consequently, it is not a requirement to

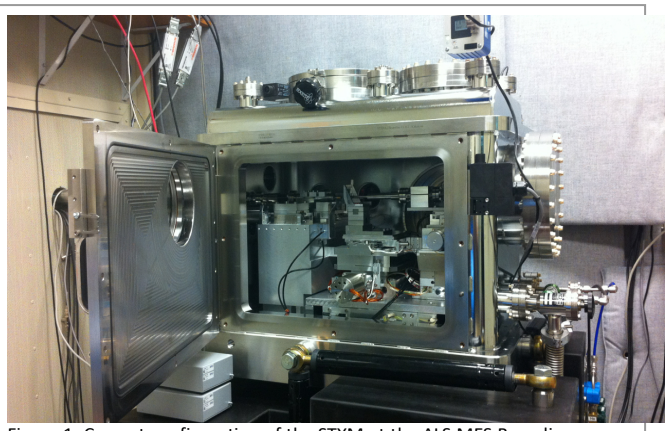

Figure 1. Current configuration of the STXM at the ALS MES Beamline.

prepare samples for high vacuum compatibility, and sample changes are relatively rapid. To operate at ambient pressure, the microscope chamber is typically purged with helium prior to data collection to prevent attenuation of the soft X-ray beam.

Experiments with dispersible radioactive materials (such as particulates) require the use of two Si_3N_4 windows enclosing the sample to ensure that the specimen remains contained. As the penetration depth of soft X-rays is on the order of 100 – 500 nm for most actinide materials, accurate transmission-mode XANES data generally cannot be acquired from samples thicker than 1 micron. Typically, a microgram quantity (or less) of material is used. To ensure appropriate sample thickness, coarse samples may be pulverized in a mortar and pestle before mounting. In the case of particulate materials, additional processing is often unnecessary.

2.2 Fluorescence Detection

One technical limitation of STXM is that transmission-mode X-ray absorption measurements have limited sensitivity to dilute species. Generally, the species of interest must be present at a concentration of several percent by weight to separate the absorption signal from the background. This means that some measurements with potential relevance for nuclear forensics cannot be performed in transmission mode. In particular, trace elements such as rare earths that can be useful for determining the source of the material,[4, 8] as well as trace fission products, will typically not be detected. While it is possible to non-destructively detect the presence of these constituents at sub-percent concentrations by X-ray fluorescence, or by SEM/EDX analysis,[4-5, 11] these methods do

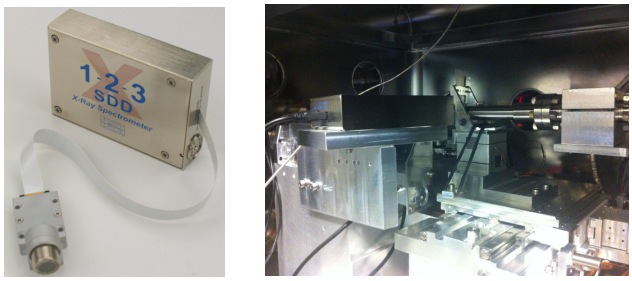

Figure 2. Left: solid state fluorescence detector (Amptek SSD) used for soft X-ray spectromicroscopy with the MES STXM. Right: mounting of the detector with respect to a STXM sample holder.

not provide full spectroscopic information.

To combine the lower detection threshold of X-ray fluorescence with the spatial resolution and spectral data available via STXM, a silicon solid-state detector has been commissioned for use with the MES instrument (Fig. 2).[35] The energy resolution of the detector (125 eV) is sufficient to separate the K-edge signals from oxygen and nitrogen, enabling K-edge spectroscopy of light atoms at concentrations of 0.5% – 1.0% by weight. It is also possible to detect lanthanides and transition metals at lower concentrations. A conservative estimate of the detection limit is 0.05 wt% for transition metals detected by L-edge derived fluorescence. Note that fluorescence yields are typically higher in the hard X-ray regime than in the soft X-ray regime,[36] and consequently the detection limit for XRF is still somewhat lower than for fluorescence-detector-coupled STXM.

2.3 Efficient Identification and Selection of Particles of Interest

For many scanning probe techniques, the amount of time needed to image and characterize a complex sample *in situ* may constitute a significant experimental bottleneck.[37] In the context of nuclear forensics, this is an important consideration since some types of nuclear materials (*e.g.*, ore materials, mixed powders, and advanced nuclear fuels) is often highly heterogeneous. Micron-scale inclusions of radionuclides may be distributed across mm-scale pieces of material.[38-41] This makes it necessary to develop strategies for efficiently identifying smaller regions of interest. Two approaches are being implemented as part of the STXM forensics effort. First, sample preparation procedures intended to efficiently isolate radioactive particles from large quantities of material are under development. Second, a software tool designed to streamline the process of STXM data collection on heterogeneous samples has been implemented at the MES STXM.

Radionuclide-rich regions of a large sample may be identified before STXM analysis by either autoradiography with an image plate reader system, or by or SEM/EDS. The choice of method depends on the sample form. Autoradiography makes it possible to easily survey large (cm-scale) sample areas, but has limited spatial resolution. SEM/EDS is often best applied to a more limited sample area, but can provide nanometer-scale spatial resolution and element-specific sensitivity. In addition, focused ion beam (FIB) milling[42] may be used in conjunction with SEM to extract thin sections of interest from a larger specimen.

For studies of heterogeneous particulate materials such as mixed powders, and for cases where sectioning or other mechanical processing is impossible, a software-assisted STXM data acquisition protocol has been developed. Typically, the process of collecting STXM data begins with a survey of a millimeter-scale area of sample at coarse resolution (> 1 micron). The user then selects regions of the sample with areas on the order of 50 × 50 microns for imaging at sub-micron resolution. Finally, smaller regions (on the order of 10 × 10 microns) are selected for imaging and spectromicroscopy at

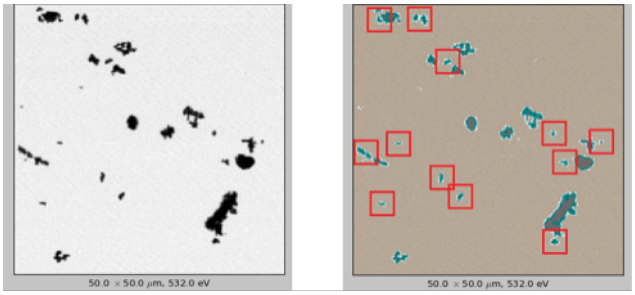

Figure 3. Screen capture from operation of the data acquisition assistance software developed for the ALS MES Beamline. Left: normal-contrast STXM image of a particulate sample. Right: processed image, indicating regions with expected thickness less than 2.0 penetration depths at photon energy 532.0 eV (i.e., above the oxygen K-edge).

resolutions ranging approximately between 25 nm and 100 nm. The choice of a particular region for inspection at high resolution depends on the presence of the element of interest and the thickness of the material; sample regions thicker than approximately 1 penetration depth at the absorption maximum yield distorted spectra. The process of searching for an appropriate region varies considerably depending on sample morphology and operator experience, and several hours of beam time may be required to manually locate a suitable particle.

With this in mind, a software tool has been developed to streamline the process of surveying a heterogeneous sample. In Fig. 3, a screenshot taken from operation of this software shows a normal-contrast STXM image together with a processed version. To generate the processed image, a convolutional neural network has been used to upsample and filter the user-provided image, generating a hypothetical higher-resolution image.[43] The sample material has been segmented from the background, and particles predicted to satisfy user-defined criteria for elemental composition and optical density have been highlighted as suggested regions for high-resolution inspection. Testing of this software has been carried out at the ALS-MES STXM and the Canadian Light Source 10ID-1 STXM.[44] In a test on a model particulate sample (Fe_2O_3), the prediction procedure suggested 72 particles for high-resolution inspection; of these, 21 were categorized as false positives due to either high optical density or insufficient useful cross-sectional area. Note that false positive rates are likely to depend on sample morphology, as the neural network was trained using images of particulate materials. The code is available by request.[45]

3. Results of Initial Nuclear Forensic Studies with the ALS-MES STXM

3.1. Compilation of Baseline Soft X-ray Absorption Data on Uranium Materials

Uranium, a naturally occurring element with fissionable isotopes, is often a target of nuclear forensic investigations. Soft X-ray XANES, particularly at the oxygen K-edge, provides

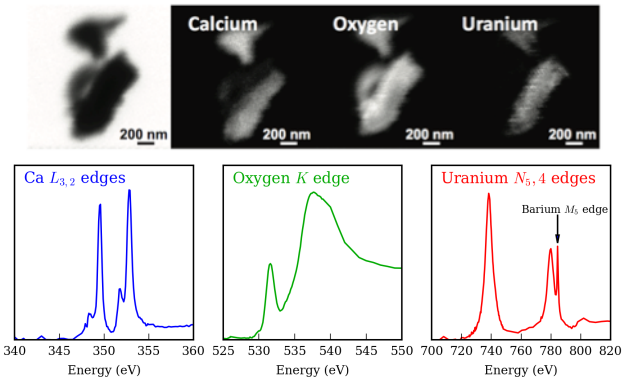

Figure 4. STXM analysis of particles of autunite (hydrated calcium uranium phosphate). Top: normal contrast image and elemental maps. Bottom: soft X-ray absorption spectra.

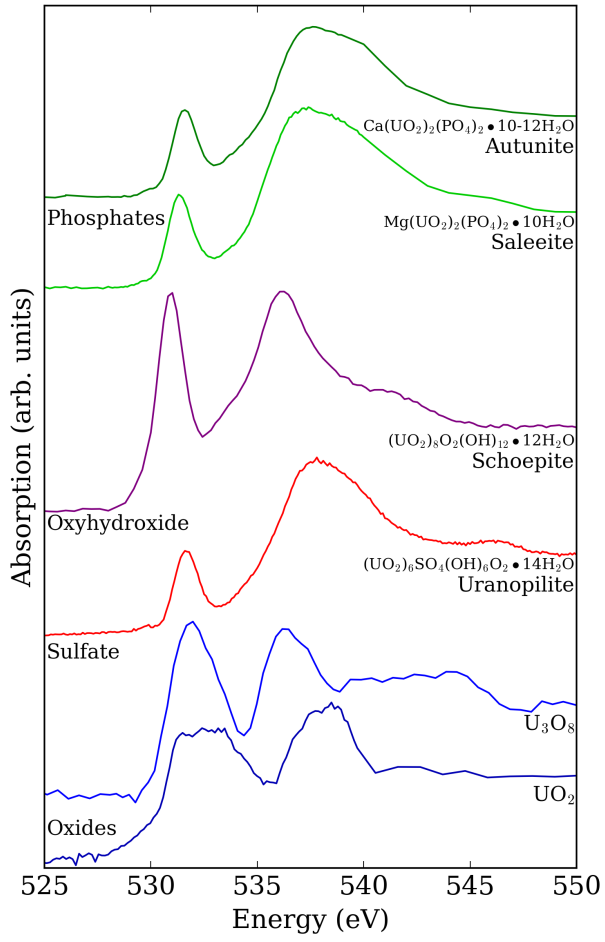

Figure 5. Oxygen K-edge spectra acquired from representative uranium compounds and minerals.

sensitive spectral fingerprints of the chemical state of uranium.[28, 30, 46-47] A comprehensive library of spectra collected from common uranium materials has been compiled from measurements at the ALS-MES STXM and literature sources. Examples are shown in Figs. 4 and 5. Fig. 4 shows a "normal contrast" image (an image acquired at a fixed photon energy, with pixel values corresponding to transmitted X-ray intensity), elemental maps, and spectra from constituent atoms collected from a single particle of autunite [$Ca(UO_2)_2(PO_4)_2 \cdot (H_2O)_x$]. The normal contrast image provides initial information about particle morphology and helps determine which particles are suitable for additional analysis. Elemental maps are generated by acquiring images at energies below and above an absorption edge of the targeted element and calculating the change in optical density at each pixel. Here, the correlation between the three elemental maps confirms that the selected particles are autunite (rather than a contaminant).

In Fig. 5, the oxygen K-edge spectrum acquired from the autunite sample is compared with spectra acquired from other uranium-bearing phases. Variations in oxygen 2p orbital structure lead to clear variations in the spectral features. In particular, uranyl compounds can often be identified by the prominent pre-edge feature near 532 eV associated with the strong U-O π interaction. Uranium oxides, on the other hand, can be identified by the width of the pre-edge peak. It should be noted that there are often significant inconsistencies from study to study in spectra collected from, for example, UO_2.[47-48] Notable publications of large XANES datasets on bulk uranium materials[28] attribute these differences to the susceptibility of UO_2 towards formation of higher oxides (e.g., U_3O_7, U_3O_8) during long-term storage, resulting in a mixture of oxides.

Fig. 6 shows an application of oxygen K-edge spectral fingerprinting in conjunction with STXM to identify components of a heterogeneous specimen. A test sample prepared by mixing powders of UO_2 and UO_2F_2 was characterized using the MES STXM. Fig. 6a shows a group of micron-scale particles that was located and imaged by normal contrast near the onset of the F K-edge (670 eV). A map of the fluorine distribution (Fig. 6b) shows only trace amounts of fluorine spread over the sample surface, implying that the selected particles consist primarily of UO_2. The oxygen K-edge spectra collected from the sample, however, are not consistent with data acquired at MES from a stoichiometric UO_2 sample (Fig. 5). This shows that the material used to prepare the sample had oxidized while in storage. By extracting representative spectra via *k*-means clustering[49] (Fig. 6c) and comparing them with the reference data, it is possible to identify some regions of the sample as UO_3 and others as an oxide or mixture of oxides intermediate between UO_2 and U_4O_9 (Fig. 6d). This type of analysis has clear utility for, e.g., quantitative determination of the mixture of oxide phases present in an aged specimen of uranium-bearing material.[11, 23, 50-53]

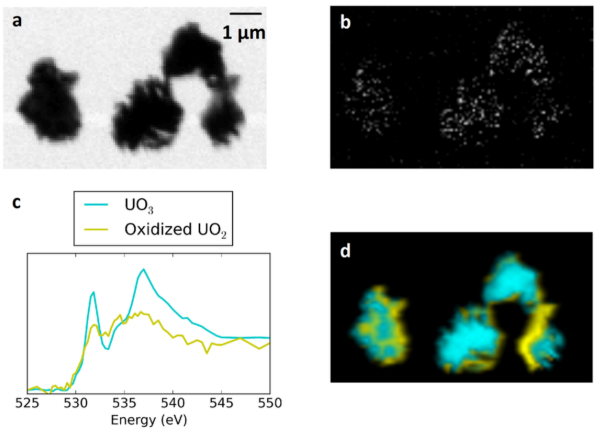

Figure 6. (a) Normal-contrast STXM image (photon energy 670 eV) of particles from a mixture of U compounds, nominally UO_2 and UO_2F_2. (b) Fluorine elemental map of the same region, showing only trace amounts of F. The selected particles are therefore predominantly composed of uranium oxide. (c) Representative spectra extracted from spatially-resolved O K-edge data by cluster analysis. Comparing these with standard U oxide spectra, one spectrum is assigned to UO_3 and the other to a uranium oxide intermediate between UO_2 and U_4O_9. (d) Image colored by similarity to the spectra shown in (c).

3.2 Melt glass speciation with soft X-ray STXM

The fallout and debris produced by the detonation of a nuclear weapon are an important category of materials of interest for nuclear forensics. Melt glass and other fallout is expected to carry information about the design and composition of the detonated device.[54-55] While there have been extensive studies of the environmental effects of weapons testing and the subsequent dispersal of radionuclides,[26, 56] there have been relatively few studies of test fallout using modern methods to improve understanding of key chemical processes such as chemical speciation.[25, 38, 41, 57-59]

A bulk-averaged hard X-ray spectroscopy study of several melt glass samples from historic nuclear tests has been recently reported.[60] Hard X-ray XANES and extended X-ray absorption fine structure (EXAFS) were used to obtain information on the oxidation state and coordination of U and Fe in each sample. Here, Fe is of interest as it is the most concentrated redox-sensitive metal in the samples, and is expected to influence the oxidation states of U and Pu.[61-63] The study shows that U in the debris (assumed to have started as some mixture of metallic and oxidized uranium) is an oxidized mixture of U(IV) and U(VI). In contrast, iron is present in the debris as strongly reduced Fe(II). These results suggest that a simple redox model is insufficient to describe the chemical speciation that occurs in nuclear melt glass formation.

A natural next step is to study the spatial distribution of Fe and U species within these materials, with the goal of more precisely describing the Fe-U redox chemistry. STXM is an ideal tool for this measurement.[64] To illustrate, Fig. 7 shows the distribution of Fe(II) and Fe(III) in a small sample of melt glass. No uranium was detected in the particular sample chosen for

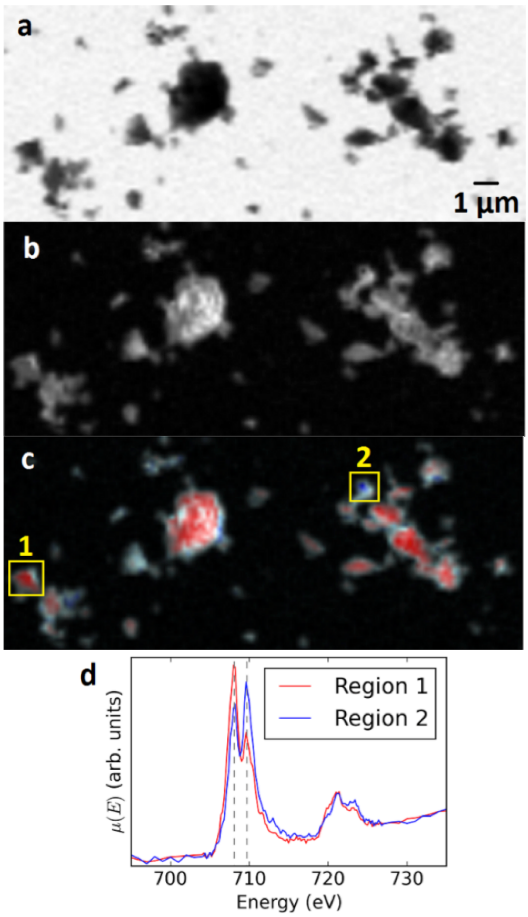

Figure 7. (a) Normal-contrast STXM image (at photon energy 745 eV) of ground nuclear test melt glass. (b) Fe elemental map. (c) Fe speciation map derived from an image stack acquired by scanning the photon energy across the Fe $L_{2,3}$ edges. For each pixel Brightness indicates Fe content as measured by the integrated intensity of the Fe L_3 edge, while color represents the Fe^{2+}/Fe^{3+} ratio as determined from the branching ratio of the Fe L_3 edge.[45,46] Red regions contain predominantly Fe^{2+} and blue regions contain predominantly Fe^{3+}. (d) Representative Fe L-edge spectra of the two regions indicated in (c). The peaks associated with Fe^{2+} (708 eV) and Fe^{3+} (709.7 eV) are marked.

STXM in this instance. The bulk-averaged concentration of U in nuclear melt glass has been reported as tens of µg/g,[38] which would be below the STXM transmission-mode detection limit if U were spread uniformly through the material. Consequently, a current priority is to select U-rich particles from a sample of melt glass by SEM, combined with X-ray fluorescence imaging and/or FIB sectioning to facilitate direct comparison of U and Fe speciation behavior. SEM studies in the literature suggest that inclusions of other metals such as copper, which may also be of interest for these studies, can be found in some glass samples with sizes ranging from nanometers to microns.[39, 41]

4. Future Prospects

The initial development of soft X-ray STXM spectromicroscopy for characterization of nuclear forensic specimens and related materials has successfully yielded valuable information, and has served to define several of the optimal capabilities and some of the limitations of the approach. This knowledge

provides direction for further forensic studies and helps define the pathway for the use and development of soft X-ray STXM for nuclear forensics applications and research in the near future. There is clearly room for additional STXM studies of materials chemistry and physics related to signatures for nuclear forensics, especially in the direction towards heavier actinide elements.

4.1 Ptychography

The equipment necessary for ptychography (diffraction-enhanced STXM imaging and spectroscopy) has been commissioned at the ALS, achieving 3 nm resolution.[65] Ptychographic capability will enable examination of speciation within single particles with nanoscale resolution, including materials such as aerosols, colloids, and other types of particles. Such information may better inform interpretations of the formation, origins, and transit pathways of nuclear material.

4.2 Access to STXM

A consideration for nuclear forensics is the availability of the MES STXM beam time (or other STXM) to efficiently conduct non-destructive analysis of a nuclear forensic specimen under realistic investigation conditions (for example, following a seizure of illicit material). Several access modes to beam time at the ALS are available, including rapid access for high-priority sample. The nuclear forensics analysis timeline set forth by the International Atomic Energy Agency for a similar analysis technique, TEM, is frequently cited as two months.[66] This is well within the capabilities of the MES STXM (unless the timing coincides with one of the regularly scheduled shutdowns of the ALS storage ring for upgrades). A programmatic stepping-stone for nuclear forensics with the STXM in the near future will be the participation in collaborative analyses of a single sample across multiple laboratories, which will test non-routine access logistics for specimen characterization by the the MES STXM.

5. Conclusions

The soft X-ray MES STXM at Beamline 11.0.2 STXM is being successfully developed for nuclear forensic materials characterization applications involving the non-destructive, analytical speciation of small radioactive particles and materials. The technical development of the MES STXM for nuclear forensics studies has resulted in significant performance improvements in fluorescence detection, sample handling, and STXM data acquisition and control system, all of which are vital components to enable various aspects of sample characterization. Preliminary nuclear forensics studies at the MES STXM have examined material signatures using XANES from actinide materials at the $N_{4,5}$-edges, from light atom constituents at the K-edges for both complexes and environmental matrices, and other relevant X-ray absorption edges residing in the soft X-ray region. We have also demonstrated the utility of these methods to the detailed investigation of spatially-related chemistry and physics in melt glass samples from nuclear testing.

Soft X-ray STXM spectromicroscopy results provide unique information that is complementary to the elemental, isotopic, and morphological data gathered using existing, established nuclear forensic techniques. There is substantial room for continued technical improvement of STXM to further optimize its capabilities for nuclear forensics studies. The current thrust of the soft X-ray STXM spectromicroscopy effort is to integrate the technique with existing forensic research, establish collaborative relationships, and continue to develop and demonstrate the value of soft X-ray STXM for the forensics community.

Conflict of interest

There are no conflicts of interest to declare.

6. Acknowledgments

This work was supported by the NNSA Office of Defense Nuclear Nonproliferation R&D (NA-22) of the U.S. Department of Energy (DOE) under Contract Number DE-AC02-05CH11231 at Lawrence Berkeley National Laboratory (LBNL) (JIP, CHB, DKS) and under Contract Number DE-AC52-07NA27344 at Lawrence Livermore National Laboratory (KBK, KSH, MJK). Additional U.S. DOE support under Contract Number DE-AC02-05CH11231 at LBNL was provided by the Director, Office of Science, Office of Basic Energy Sciences, Division of Chemical Sciences, Geosciences, and Biosciences Condensed Phase and Interfacial Molecular Sciences Program (ALS MES Beamline and TT); and by the Director, Office of Science, Office of Basic Energy Sciences, Division of Chemical Sciences, Geosciences, and Biosciences Heavy Element Chemistry Program (SGM). ABA acknowledges support a DOE Integrated University Program Fellowship at the University of California, Berkeley. Funding for this work was provided by the Department of Energy/National Nuclear Security Administration Office of Nuclear Controls (NA-242) and utilized capabilities developed with funding from Department of Energy/National Nuclear Security Administration Office of Nuclear Noncompliance Verification (NA-243). LLNL-JRNL-704342

7. References

1. Moody, K. J.; Hutcheon, I. D.; Grant, P. M., *Nuclear Forensic Analysis*. 2nd ed.; CRC Press: Boca Raton, FL, 2015; p xxii, 502 pages.
2. Kristo, M. J.; Tumey, S. J., The state of nuclear forensics. *Nuclear Instruments and Methods in Physics Research, Section B: Beam Interactions with Materials and Atoms* **2013,** *294*, 656-661.
3. Mayer, K.; Wallenius, M.; Varga, Z., Nuclear forensic science: correlating measurable material parameters to the history of nuclear material. *Chemical Reviews* **2013,** *113*, 884-900.
4. Mayer, K.; Wallenius, M.; Lützenkirchen, K.; Galy, J.; Varga, Z.; Erdmann, N.; Buda, R.; Kratz, J.-V.; Trautmann, N.; Fifield, K.,

Nuclear Forensics: A Methodology Applicable to Nuclear Security and to Non-Proliferation. *Journal of Physics: Conference Series* **2011,** *312*, 062003.

5. Mayer, K.; Wallenius, M.; Ray, I., Nuclear forensics--a methodology providing clues on the origin of illicitly trafficked nuclear materials. *The Analyst* **2005,** *130*, 433-441.

6. Wallenius, M.; Lützenkirchen, K.; Mayer, K.; Ray, I.; de las Heras, L. A.; Betti, M.; Cromboom, O.; Hild, M.; Lynch, B.; Nicholl, A.; Ottmar, H.; Rasmussen, G.; Schubert, A.; Tamborini, G.; Thiele, H.; Wagner, W.; Walker, C.; Zuleger, E., Nuclear forensic investigations with a focus on plutonium. *Journal of Alloys and Compounds* **2007,** *444-445*, 57-62.

7. Grant, P. M.; Moody, K. J.; Hutcheon, I. D.; Phinney, D. L.; Whipple, R. E.; Haas, J. S.; Alcaraz, A.; Andrews, J. E.; Klunder, G. L.; Russo, R. E.; Fickies, T. E.; Pelkey, G. E.; Andresen, B. D.; Kruchten, D. A.; Cantlin, S., Nuclear forensics in law enforcement applications. *Journal of Radioanalytical and Nuclear Chemistry* **1998,** *235*, 129-132.

8. Grant, P. M.; Moody, K. J.; Hutcheon, I. D.; Phinney, D. L.; Haas, J. S.; Volpe, A. M.; Oldani, J. J.; Whipple, R. E.; Stoyer, N.; Alcaraz, A.; Andrews, J. E.; Russo, R. E.; Klunder, G. L.; Andresen, B. D.; Cantlin, S., Forensic Analyses of Suspect Illicit Nuclear Material. *Journal of Forensic Science* **1998**, 680-688.

9. Wallenius, M.; Mayer, K.; Ray, I., Nuclear forensic investigations: Two case studies. *Forensic Sci Int* **2006,** *156*, 55-62.

10. Keegan, E.; Kristo, M. J.; Colella, M.; Robel, M.; Williams, R.; Lindvall, R.; Eppich, G.; Roberts, S.; Borg, L.; Gaffney, A.; Plaue, J.; Wong, H.; Davis, J.; Loi, E.; Reinhard, M.; Hutcheon, I., Nuclear forensic analysis of an unknown uranium ore concentrate sample seized in a criminal investigation in Australia. *Forensic Sci Int* **2014,** *240*, 111-121.

11. Kristo, M. J.; Keegan, E.; Colella, M.; Williams, R.; Lindvall, R.; Eppich, G.; Roberts, S.; Borg, L.; Gaffney, A.; Plaue, J.; Knight, K.; Loi, E.; Hotchkis, M.; Moody, K.; Singleton, M.; Robel, M.; Hutcheon, I., Nuclear forensic analysis of uranium oxide powders interdicted in Victoria, Australia. *Radiochim Acta* **2015,** *103* (7), 487-500.

12. Bellucci, J. J.; Simonetti, A.; Wallace, C.; Koeman, E. C.; Burns, P. C., Lead Isotopic Composition of Trinitite Melt Glass: Evidence for the Presence of Canadian Industrial Lead in the First Atomic Weapon Test. *Anal Chem* **2013,** *85*, 7588-7593.

13. Bellucci, J. J.; Simonetti, A.; Wallace, C.; Koeman, E. C.; Burns, P. C., Isotopic Fingerprinting of the World's First Nuclear Device Using Post-Detonation Materials. *Anal Chem* **2013,** *85*, 4195-4198.

14. Betti, M.; Tamborini, G.; Koch, L., Use of secondary ion mass spectrometry in nuclear forensic analysis for the characterization of plutonium and highly enriched uranium particles. *Anal Chem* **1999,** *71*, 2616-2622.

15. Hou, X.; Chen, W.; He, Y.; Jones, B. T., Analytical Atomic Spectrometry for Nuclear Forensics. *Applied Spectroscopy Reviews* **2005,** *40*, 245-267.

16. Ranebo, Y.; Eriksson, M.; Tamborini, G.; Niagolova, N.; Bildstein, O.; Betti, M., The use of SIMS and SEM for the characterization of individual particles with a matrix originating from a nuclear weapon. *Microscopy Microanal* **2007,** *13*, 179-90.

17. Tamborini, G., SIMS Analysis of Uranium and Actinides in Microparticles of Different Origin. *Microchimica Acta* **2004,** *145*, 237-242.

18. Tamborini, G.; Wallenius, M.; Bildstein, O.; Pajo, L.; Betti, M., Development of a SIMS method for isotopic measurements in nuclear forensic applications. *Microchimica Acta* **2002,** *139*, 185-188.

19. Duff, M. C.; Coughlin, J. U.; Hunter, D. B., Uranium co-precipitation with iron oxide minerals. *Geochimica et Cosmochimica Acta* **2002,** *66*, 3533-3547.

20. Hess, N. J.; Weber, W. J.; Conradson, S. D., X-ray absorption fine structure of aged, Pu-doped glass and ceramic waste forms. *Journal of Nuclear Materials* **1998,** *254*, 175-184.

21. Jollivet, P.; Auwer, C. D.; Simoni, E., Evolution of the uranium local environment during alteration of SON68 glass. *Journal of Nuclear Materials* **2002,** *301*, 142-152.

22. Pacold, J. I.; Lukens, W. W.; Booth, C. H.; Shuh, D. K.; Knight, K. B.; Eppich, G. R.; Holliday, K. S., Chemical speciation of U, Fe, and Pu in melt glass from nuclear weapons testing. *Journal of Applied Physics* **2016,** *119*, 195102.

23. Crean, D. E.; Livens, F. R.; Stennett, M. C.; Grolimund, D.; Borca, C. N.; Hyatt, N. C., Microanalytical X-ray Imaging of Depleted Uranium Speciation in Environmentally Aged Munitions Residues. *Environmental Science & Technology* **2014,** *48*, 1467-1474.

24. Tamasi, A. L.; Boland, K. S.; Czerwinski, K.; Ellis, J. K.; Kozimor, S. A.; Martin, R. L.; Pugmire, A. L.; Reilly, D.; Scott, B. L.; Sutton, A. D.; Wagner, G. L.; Walensky, J. R.; Wilkerson, M. P., Oxidation and Hydration of U 3 O 8 Materials Following Controlled Exposure to Temperature and Humidity. *Anal Chem* **2015,** *87*, 4210-4217.

25. Giuli, G.; Pratesi, G.; Eeckhout, S. G.; Paris, E., Iron reduction in silicate glass produced during the 1945 nuclear test at the Trinity site (Alamogordo, New Mexico, USA). *Large Meteorite Impacts and Planetary Evolution IV* **2010,** *465*.

26. Rose, T. P.; Kersting, a. B.; Harris, L. J.; Hudson, G. B.; Smith, D. K.; Williams, R. W.; Loewen, D. R.; Nelson, E. J.; Moran, J. E. *Hydrologic Resources Management Program and Underground Test Area Project FY 2001 – 2002 Progress Report*; 2003.

27. Solomon, E. I.; Hedman, B.; Hodgson, K. O.; Dey, A.; Szilagyi, R. K., Ligand K-edge X-ray absorption spectroscopy: covalency of ligand–metal bonds. *Coordination Chemistry Reviews* **2005,** *249*, 97-129.

28. Ward, J. D.; Bowden, M.; Resch, C. T.; Smith, S.; McNamara, B. K.; Buck, E. C.; Eiden, G. C.; Duffin, A. M., Identification of Uranyl Minerals Using Oxygen K-Edge X-Ray Absorption Spectroscopy. *Geostandards and Geoanalytical Research* **2015,** *40* (1), 135-148.

29. Minasian, S. G.; Keith, J. M.; Batista, E. R.; Boland, K. S.; Clark, D. L.; Kozimor, S. a.; Martin, R. L.; Shuh, D. K.; Tyliszczak, T., New evidence for 5f covalency in actinocenes determined from carbon K-edge XAS and electronic structure theory. *Chemical Science* **2014,** *5*, 351.

30. Wen, X.-D.; Löble, M. W.; Batista, E. R.; Bauer, E.; Boland, K. S.; Burrell, A. K.; Conradson, S. D.; Daly, S. R.; Kozimor, S. a.; Minasian, S. G.; Martin, R. L.; McCleskey, T. M.; Scott, B. L.; Shuh, D. K.; Tyliszczak, T., Electronic structure and O K-edge XAS spectroscopy of U3O8. *Journal of Electron Spectroscopy and Related Phenomena* **2014,** *194*, 81-87.

31. Bluhm, H.; Andersson, K.; Araki, T.; Benzerara, K.; Brown, G. E.; Dynes, J. J.; Ghosal, S.; Gilles, M. K.; Hansen, H. C.; Hemminger, J. C.; Hitchcock, A. P.; Ketteler, G.; Kilcoyne, a. L. D.; Kneedler, E.; Lawrence, J. R.; Leppard, G. G.; Majzlam, J.; Mun, B. S.; Myneni, S. C. B.; Nilsson, a.; Ogasawara, H.; Ogletree, D. F.; Pecher, K.; Salmeron, M.; Shuh, D. K.; Tonner, B.; Tyliszczak, T.; Warwick, T.; Yoon, T. H. In *Soft X-ray microscopy and spectroscopy at the molecular environmental science beamline at the Advanced Light Source*, AIP Conference Proceedings, 2004; pp 86-104.

32. Kilcoyne, A. L. D.; Tyliszczak, T.; Steele, W. F.; Fakra, S.; Hitchcock, P.; Franck, K.; Anderson, E.; Harteneck, B.; Rightor, E. G.; Mitchell, G. E.; Hitchcock, A. P.; Yang, L.; Warwick, T.; Ade, H., Interferometer-controlled scanning transmission X-ray microscopes

at the Advanced Light Source. *J Synchrotron Radiat* **2003,** *10*, 125-136.
33. Tyliszczak, T. In *Soft X-ray Scanning Transmission Microscope Working in an Extended Energy Range at the Advanced Light Source*, AIP Conference Proceedings, 2004; pp 1356-1359.
34. de Groot, F. M. F.; de Smit, E.; van Schooneveld, M. M.; Aramburo, L. R.; Weckhuysen, B. M., In-situ scanning transmission X-ray microscopy of catalytic solids and related nanomaterials. *Chemphyschem* **2010,** *11*, 951-62.
35. Hitchcock, A. P.; Obst, M.; Wang, J.; Lu, Y. S.; Tyliszczak, T., Advances in the Detection of As in Environmental Samples Using Low Energy X-ray Florescence in a Scanning Transmission X-Ray Microscope: Arsenic Immobilization by a Fe(II)-Oxidizing Freshwater Bacteria. *Environmental Science & Technology* **2012,** *46*, 2821-9.
36. Krause, M. O., Atomic radiative and radiationless yields for K and L shells. *Journal of Physical and Chemical Reference Data* **1979,** *8*, 307.
37. Kotula, P. G.; Keenan, M. R.; Michael, J. R., Automated analysis of SEM X-ray spectral images: a powerful new microanalysis tool. *Microscopy Microanal* **2003,** *9*, 1-17.
38. Eppich, G. R.; Knight, K. B.; Jacomb-Hood, T. W.; Spriggs, G. D.; Hutcheon, I. D., Constraints on fallout melt glass formation from a near-surface nuclear test. *Journal of Radioanalytical and Nuclear Chemistry* **2014,** *302*, 593-609.
39. Eby, G. N.; Charnley, N.; Pirrie, D.; Hermes, R.; Smoliga, J.; Rollinson, G., Trinitite redux : Mineralogy and petrology. *American Mineralogist* **2015,** *100*, 427-441.
40. Eby, N.; Hermes, R.; Charnley, N.; Smoliga, J., Trinitite—the atomic rock. *Geology Today* **2010,** *26*, 180-185.
41. Fahey, A. J.; Zeissler, C. J.; Newbury, D. E.; Davis, J.; Lindstrom, R. M., Postdetonation nuclear debris for attribution. *Proceedings of the National Academy of Sciences* **2010,** *107*, 20207-20212.
42. Volkert, C. A.; Minor, A. M., Focused Ion Beam Microscopy and Micromachining. *MRS Bulletin* **2007,** *32*, 389-399.
43. Dong, C.; Loy, C. C.; He, K. M.; Tang, X. O., Image Super-Resolution Using Deep Convolutional Networks. *IEEE Trans Pattern Anal* **2016,** *38* (2), 295-307.
44. Kaznatcheev, K. V.; Karunakaran, C.; Lanke, U. D.; Urquhart, S. G.; Obst, M.; Hitchcock, A. P., Soft X-ray spectromicroscopy beamline at the CLS: Commissioning results. *Nuclear Instruments and Methods in Physics Research Section A: Accelerators, Spectrometers, Detectors and Associated Equipment* **2007,** *582*, 96-99.
45. Pacold, J. I. STXM Live Analysis. https://github.com/jpacold/STXM_live/.
46. Conradson, S. D.; Durakiewicz, T.; Espinosa-Faller, F. J.; An, Y. Q.; Andersson, D. A.; Bishop, A. R.; Boland, K. S.; Bradley, J. A.; Byler, D. D.; Clark, D. L.; Conradson, D. R.; Conradson, L. L.; Costello, A. L.; Hess, N. J.; Lander, G. H.; Llobet, A.; Martucci, M. B.; de Leon, J. M.; Nordlund, D.; Lezama-Pacheco, J. S.; Proffen, T. E.; Rodriguez, G.; Schwarz, D. E.; Seidler, G. T.; Taylor, A. J.; Trugman, S. A.; Tyson, T. A.; Valdez, J. A., Possible Bose-condensate behavior in a quantum phase originating in a collective excitation in the chemically and optically doped Mott-Hubbard system UO2+x. *Phys Rev B* **2013,** *88* (11).
47. Nilsson, H. J.; Tyliszczak, T.; Wilson, R. E.; Werme, L.; Shuh, D. K., Soft X-ray scanning transmission X-ray microscopy (STXM) of actinide particles. *Analytical and Bioanalytical Chemistry* **2005,** *383*, 41-7.
48. Kalkowski, G.; Kaindl, G.; Brewer, W.; Krone, W., Near-edge x-ray-absorption fine structure in uranium compounds. *Phys Rev B* **1987,** *35*, 2667-2677.
49. Lerotic, M.; Jacobsen, C.; Schafer, T.; Vogt, S., Cluster analysis of soft X-ray spectromicroscopy data. *Ultramicroscopy* **2004,** *100* (1-2), 35-57.
50. Senanayake, S. D.; Waterhouse, G. I. N.; Chan, A. S. Y.; Madey, T. E.; Mullins, D. R.; Idriss, H., Probing Surface Oxidation of Reduced Uranium Dioxide Thin Film Using Synchrotron Radiation. *Journal of Physical Chemistry C* **2007,** *111*, 7963-7970.
51. Senanayake, S. D.; Waterhouse, G. I. N.; Chan, A. S. Y.; Madey, T. E.; Mullins, D. R.; Idriss, H., The reactions of water vapour on the surfaces of stoichiometric and reduced uranium dioxide: A high resolution XPS study. *Catalysis Today* **2007,** *120*, 151-157.
52. Idriss, H., Surface reactions of uranium oxide powder, thin films and single crystals. *Surface Science Reports* **2010,** *65*, 67-109.
53. Tamasi, A. L.; Boland, K. S.; Czerwinski, K.; Ellis, J. K.; Kozimor, S. A.; Martin, R. L.; Pugmire, A. L.; Reilly, D.; Scott, B. L.; Sutton, A. D.; Wagner, G. L.; Walensky, J. R.; Wilkerson, M. P., Oxidation and Hydration of U ₃ O ₈ Materials Following Controlled Exposure to Temperature and Humidity. *Anal Chem* **2015,** *87*, 4210-4217.
54. Glasstone, S.; Dolan, P. J., *The Effects of Nuclear Weapons*. US Government Printing Office: Washington, 1977.
55. Freiling, E. C., Radionuclide Fractionation in Bomb Debris. *Science* **1961,** *133*, 1991-1998.
56. Kersting, A. B., Plutonium transport in the environment. *Inorganic Chemistry* **2013,** *52*, 3533-3546.
57. Cassata, W. S.; Prussin, S. G.; Knight, K. B.; Hutcheon, I. D.; Isselhardt, B. H.; Renne, P. R., When the dust settles: stable xenon isotope constraints on the formation of nuclear fallout. *Journal of Environmental Radioactivity* **2014,** *137C*, 88-95.
58. Bellucci, J. J.; Simonetti, A.; Koeman, E. C.; Wallace, C.; Burns, P. C., A detailed geochemical investigation of post-nuclear detonation trinitite glass at high spatial resolution: Delineating anthropogenic vs. natural components. *Chemical Geology* **2014,** *365*, 69-86.
59. Koeman, E. C.; Simonetti, A.; Burns, P. C., Sourcing of Copper and Lead within Red Inclusions from Trinitite Postdetonation Material. *Anal Chem* **2015,** *87*, 5380-5386.
60. Pacold, J. I.; Lukens, W. W.; Booth, C. H.; Shuh, D. K.; Knight, K. B.; Holliday, K. S., Chemical Speciation of U, Fe, and Pu in Melt Glass from Nuclear Weapons Testing. *Journal of Applied Physics* **2016,** *accepted*.
61. Schreiber, H. D., The chemistry of uranium in glass-forming aluminosilicate melts. *Journal of the Less Common Metals* **1983,** *91*, 129-147.
62. Schreiber, H. D., Properties of redox ions in glasses: An interdisciplinary perspective. *Journal of Non-Crystalline Solids* **1980,** *42*, 175-183.
63. Schreiber, H. D.; Kochanowski, B. K.; Schreiber, C. W.; Morgan, A. B.; Coolbaugh, M. T.; Dunlap, T. G., Compositional dependence of redox equilibria in sodium silicate glasses. *Journal of Non-Crystalline Solids* **1994,** *177*, 340-346.
64. Bourdelle, F.; Benzerara, K.; Beyssac, O.; Cosmidis, J.; Neuville, D. R.; Brown, G. E.; Paineau, E., Quantification of the ferric/ferrous iron ratio in silicates by scanning transmission X-ray microscopy at the Fe L2,3 edges. *Contributions to Mineralogy and Petrology* **2013,** *166*, 423-434.
65. Shapiro, D. A.; Yu, Y.-S.; Tyliszczak, T.; Cabana, J.; Celestre, R.; Chao, W.; Kaznatcheev, K.; Kilcoyne, A. L. D.; Maia, F.; Marchesini, S.; Meng, Y. S.; Warwick, T.; Yang, L. L.; Padmore, H. A., Chemical composition mapping with nanometre resolution by soft X-ray microscopy. *Nature Photonics* **2014**, 1-5.
66. Nuclear Forensics in Support of Investigations. Vienna, 2015; Vol. 2-G.

1